



One-Step Spontaneous Formation of Dual Wrinkling on Uniform-Sized Microparticles Induced by Surface

Jinsol Im, Dongik Yoo, Jihoon Kim, Sukeun Yoon,* and Kuk Young Cho*

This study demonstrates the wrinkle formation on biodegradable polymer-blend microparticles prepared from an emulsion-solvent evaporation method and investigates the formed patterns. A labyrinthine pattern is obtained for uniform-sized microparticles, owing to the considerable size reduction during solvent evaporation. Changing the radius of the organic droplets dispersed in the aqueous solution switches the wrinkle pattern from labyrinth to bi-phase. For the first time, the dual wrinkling structure is prepared; both labyrinthine texture and hexagonal dimple structures are spontaneously formed on the same microparticle surface. The former pattern is due to the surface instability from blends of hydrophobic polymer and amphiphilic block copolymer, while the latter is due to a mechanism similar that of the breath figure formed with organic phase change materials during solidification of microparticles. The general applicability of this approach is demonstrated on other pairs of polymer blends.

1. Introduction

Microparticles with wrinkled surfaces are widely found in nature (e.g., seeds, pollen grains, and microorganisms),^[1–4] and the wrinkles affect the physical properties of particles through the enlarged surface areas. Despite the short history of studying buckling formation on substrate with curvature,^[5] wrinkling on curved substrates and microparticles have shown promising applications in many fields, such as nanoscale surface patterning,^[6] microlens array fabrication,^[7] emerging micro-fingerprinting technique,^[8] and adaptive aerodynamic drag control.^[9,10] Thus, the formation of wrinkles on the polymeric microparticles is attracting considerable interest.

The theory and experiments on the buckling pattern on curved substrates were first studied for the Ag core/SiO₂

shell system.^[5] Li et al. explained surface buckling and morphological transition of a core-shell soft sphere based on a volumetric growth theory of finite deformation.^[11] Recently, the mechanism of forming and selecting the wrinkle pattern on curved surfaces has been visualized using a curved elastic ball with bilayer surface, through a pneumatic device that controls the pressure in the cavity inside the ball.^[12,13]

The biomimetic approach of creating wrinkles on uniform-sized microparticles of biocompatible polymer is suitable for reproducibly fabricating tailor-made functional microparticles.^[14] The emulsion-solvent evaporation method has been widely used to fabricate microparticles. However, there is a lack of adequate understanding of the wrinkle formation during solvent

evaporation, as well as the determination of the wrinkle pattern.

Two parallel routes, namely the adapting technique and surface instability approach, have been used to accomplish micro- and nanopatterns on surfaces.^[15] The former generally treats formed microparticles with chemical and physical processes to induce surface wrinkling, whereas the latter approach uses the inherent properties of materials to induce particular surface patterns, such as phase separation of polymer blends, breath figures, and thermal-gradient-induced surface patterning.

Considering the materials for wrinkled microparticle fabrication, poly(dimethyl siloxane) (PDMS)^[16,17] and elastomeric crosslinked polymer^[18,19] that are stable for the adapting technique (e.g., UV irradiation) have been prepared into wrinkled microparticles. However, biocompatible polymers based on aliphatic polyesters have poorer mechanical and thermal stability compared to PDMS. Thus, spontaneous wrinkle formation via surface instability seems the more promising route for biocompatible polymer particles.

The microfluidic droplet formation approach could produce microparticles with a narrow size distribution. However, the needs for flow control or/and UV curing limit the choice of materials for anisotropic microparticles.^[20,21] Recently, we fabricated aspherical microparticles based on immiscible polymer blends. This provides the possibility of modifying the shape of the uniform-sized microparticles.^[22] Therefore, we consider these biodegradable polymer blends as promising source materials for manufacturing uniform-sized, wrinkled microparticles from a microfluidic device.

In addition to the cases of one simple pattern, some biological particles show multiple surface patterns

J. Im, D. Yoo, Prof. K. Y. Cho
Department of Materials Science and Chemical Engineering
Hanyang University
55 Hanyangdaehak-ro, Sangrok-gu, Gyeonggi 15588, Korea
E-mail: kycho@hanyang.ac.kr; chokukyoung@gmail.com

Prof. J. Kim, Prof. S. Yoon
Division of Advanced Materials Engineering
Kongju National University
1223-24 Cheonan-daero
Seobuk-gu, Cheonan, Chungnam 31080, Korea
E-mail: skyoon@kongju.ac.kr

The ORCID identification number(s) for the author(s) of this article can be found under <https://doi.org/10.1002/macp.201700152>.

DOI: 10.1002/macp.201700152

(e.g., *P. mooreana* pollen).^[4] Unfortunately, dual-wrinkled microparticles are much unexplored in research because of the difficulty of their fabrication, and dual wrinkling on uniform-sized microparticles of biocompatible polymers has not been reported to the best of our knowledge. Herein, we investigated the wrinkle formation during the fabrication of these particles using the emulsion-solvent evaporation method. We also demonstrated the dual wrinkling (labyrinthine and hexagonal phases) on the same surface of uniform-sized microparticles using biodegradable polymer for the first time.

2. Experimental Section

2.1. Materials

Poly(D,L-lactide-co-glycolide) (PLGA, D,L-lactide:glycolide = 65:35, η_{inh} : 0.55–0.75 dl g⁻¹ in hexafluoroisopropanol, Lactel) was used as a main component in the polymer blend. The amphiphilic block copolymers poly(ϵ -caprolactone)-*b*-poly(ethylene glycol) diblock copolymer (PCL-*b*-mPEG), poly(ϵ -caprolactone)-*b*-poly(ethylene glycol)-*b*-poly(ϵ -caprolactone) triblock copolymer (PCL-*b*-PEG-*b*-PCL), and poly(D,L-lactide)-*b*-poly(ethylene glycol) diblock copolymer (PDLA-*b*-mPEG) were synthesized using stannous octoate (Sigma) as a catalyst via ring-opening polymerization. Monomethoxy-terminated poly(ethylene glycol) (mPEG, M_w = 2000) and poly(ethylene glycol) (PEG, M_w = 6000) were used as a macroinitiator for diblock and triblock copolymers, respectively. Briefly, fully dried mPEG or PEG was placed in the 20 mL vial reactor and heated up to 140 °C. Stannous octoate diluted using toluene was introduced in the reactor, and the amount of catalyst was 0.4 wt% of PEG. Together with the catalyst, monomer ϵ -caprolactone was also introduced and reaction proceeded for 6 h at 140 °C. After the reaction, the product was dissolved in dichloromethane (DCM) and precipitated using excess of petroleum ether. Synthesized polymer was washed three times using petroleum ether and fully dried in vacuum for 24 h. 2-Methylpentane (TCl, Japan) was used as an inert organic volatile phase change material (PCM) for generating surface dimples and internal pore structure of microparticles.

2.2. Fabrication of Microparticles

A tube-type microfluidic device was used to prepare wrinkled microparticles with a narrow distribution. Detailed description of the fluid-type setting for fabricating microparticles in this device could be found in our previous research.^[23] The continuous flow was 1 wt% poly(vinyl alcohol) (PVA, 87–89% hydrolyzed, M_w = 13 000–23 000, Aldrich) aqueous solution. The oil phase discontinuous flow comprised of polymer dissolved in DCM where the concentration was 10 wt%. The blend ratios of PLGA and PCL-*b*-mPEG were 9:1, 8:2, 7:3, and 6:4. To fabricate dual-wrinkled microparticles, the organic solution contained polymer blend and 2-methylpentane at the ratio of 7:3, maintaining a solution concentration of 10 wt%.

2.3. Instrumentation

Interfacial tension between the oil/aqueous phase solutions for various blending ratios was measured by a surface tension analyzer (DST60, SEO, Korea), which worked by the du Noüy ring method. The oil drops that composed of polymers and PCM dissolved in DCM were observed by using an optical microscope (Leica DMIL, USA) equipped with a digital camera. The scanning electron microscopy (SEM) images of microparticles were obtained by imaging Pt-sputtered particles on top of the carbon tape, and measurements were done by using an accelerating voltage of 15.0 kV in a field-emission SEM (FE-SEM, MIRA-3, Tescan). The viscosity of various polymer solutions was measured at 25 °C using a viscometer (μ VISC, RheoSense) with the sensor model HA-01-01.

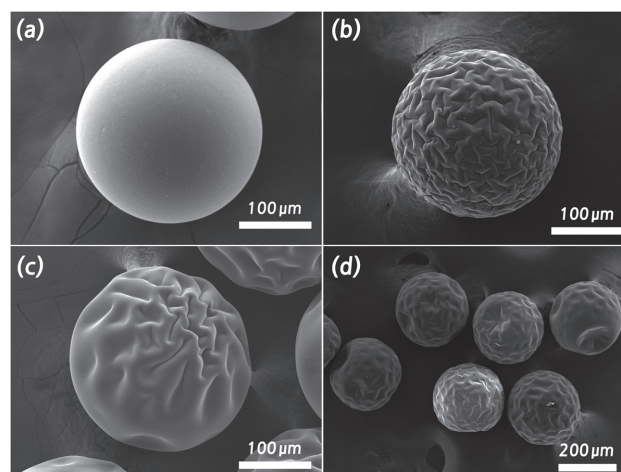


Figure 1. Surface morphology of microparticles from blends of PLGA/PCL-*b*-mPEG formed from the tube-type fluidic device, with different blend ratios: a) 9:1, b) 8:2, and c) 7:3. d) Multiple particles of (b) showing size uniformity.

3. Results and Discussion

Amphiphilic block copolymers containing both hydrophobic and hydrophilic groups are an interesting class of polymeric materials that exhibit a rich variety of morphologies in the blend. We have synthesized amphiphilic PCL-*b*-mPEG copolymer, and its structure was confirmed by ¹H NMR spectra (Figure S1, Supporting Information). The weight-average molecular weight (M_w) was 16 200 (Table S1, Supporting Information), and the melting temperature was 54.23 °C (Figure S2, Supporting Information). PLGA was selected as a hydrophobic polymer in the blend owing to its wide use as a biocompatible polymer. Microparticles were prepared with varying blend ratios of PLGA:PCL-*b*-mPEG being 9:1, 8:2, 7:3 (wt%), with PLGA being the main matrix (Figure 1). Continuous flow rate of 100 mL·h⁻¹ and discontinuous flow at 0.1 mL·h⁻¹ was used to fabricate microparticle in fluidic device.

When the composition of PCL-*b*-mPEG in the blend exceeds 40 wt% (i.e., 6:4 ratio), the formed particles are sticky and lose their structural integrity during the drying procedure. Labyrinthine morphology on the surface of the microparticles was observed when the composition of amphiphilic copolymer exceeds 20 wt% in the polymer blend.

The surface wrinkling can be observed when a critical condition is satisfied. This critical shrinking factor is influenced by the ratio between the shear moduli of the shell and the inner layer. When this ratio is small, large shrinking factor value is needed for wrinkling. Spontaneous wrinkling occurs in order to minimize the combined bending energy of the outer layer and stretching energy of the inner layer.^[17] The result shows that wrinkles induced by phase separation are effective for blends containing sufficient amount of amphiphilic copolymer.

Because the microparticles are prepared from a microfluidic device, they can have similar sizes despite the wrinkled surface (Figure 1d).

The wrinkling morphology and pattern selection in curved elastic bilayer (stiff film on a soft substrate) materials can

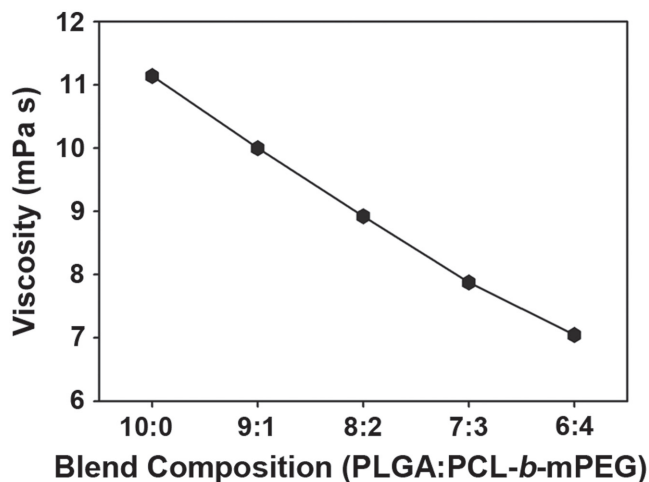


Figure 2. Viscosities of the polymer blend dissolved in DCM where the total polymer concentration was fixed to 10 wt%.

be described by the generalized Swift-Hohenberg theory.^[12] Depending on the surface instability, hexagonal, bistable, and labyrinthine phase could be formed. Generally, labyrinthine phases were largely observed from the wrinkled microparticle. The formation of labyrinthine phase was also favorable for wrinkled microparticles based on the surface instability from our fabrication condition.

Figure 2 shows the effect of blend composition on the solution viscosities. Clearly, the viscosity of the blend dissolved in DCM decreased with increasing content of amphiphilic block copolymer content, whose PEG section lowers the viscosity. Therefore, we expect that adding the amphiphilic block copolymer will facilitate polymer chain movement inside the organic solution.

The interfacial tension between the water (1 wt% PVA aqueous solution) and the organic phase (10 wt% of polymer blend in different compositions dissolved in DCM) was measured. As shown in **Figure 3**, the interfacial tension decreased with the increase of the PCL-*b*-mPEG diblock copolymer content in the blend. This is because the amphiphilic character of the diblock copolymer contributes to lowering the interfacial instability.^[24]

Specifically, the diblock copolymer will move to the water/organic interface to reduce the interfacial tension. This will cause surface roughening during the solidification of the organic droplet.^[25,26] **Figure 3** shows that there is a significant drop of interfacial tension between the blend ratios of 9:1 and 8:2. This is in good agreement with the clear change in surface texture between **Figure 1a,b**.

After exiting the tube-type microfluidic device, the formation of wrinkling on the surface of the organic droplets during the evaporation of DCM was directly confirmed by the optical microscopic images (**Figure 4**).

The wavelength (λ) of wrinkles can be expressed as^[19,27]

$$\lambda \approx 2\pi h \left(\frac{1}{3} \right)^{1/3} \left(\frac{E_f}{E_s} \right)^{1/3} \quad (1)$$

where h is the thickness of the stiff layer, and E_s and E_f are Young's moduli of the soft core layer and the stiff shell,

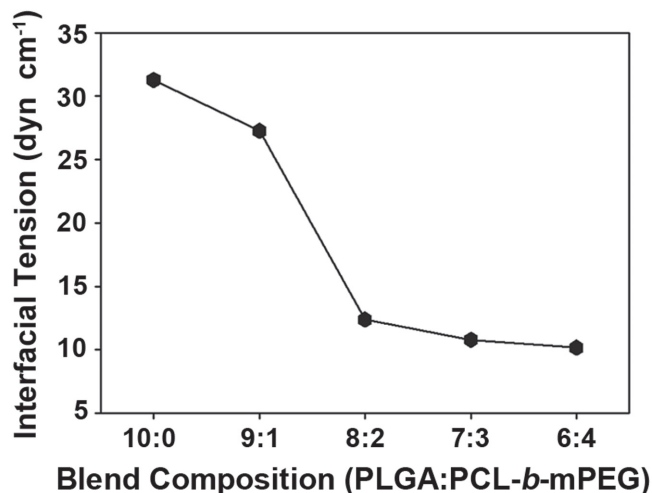


Figure 3. Effect of the blend composition (PLGA:PCL-*b*-mPEG ratio) on the interfacial tension between the organic phase (PLGA/PCL-*b*-mPEG blend dissolved in DCM) and the water phase (1 wt% PVA aqueous solution).

respectively. From the equation, a stiffer layer (higher E_f) favors a larger wrinkle wavelength, while a stiffer substrate prefers a shorter wavelength. In the optical microscopy investigation, ethanol works as a highly miscible nonsolvent for the DCM solvent and promotes the fast solvent removal at the surface of the organic phase. Hence, we have used a 1:1 mixture of ethanol and 1 wt% PVA aqueous solution as the water phase, instead of the PVA aqueous solution alone. This allows the visualization of a wavy stiff layer formed by controlled precipitation on the soft inner layer using optical microscopy, in a short period during solidification of organic droplets. An initial organic droplet containing PLGA/PCL-*b*-mPEG showed hazy interior upon its

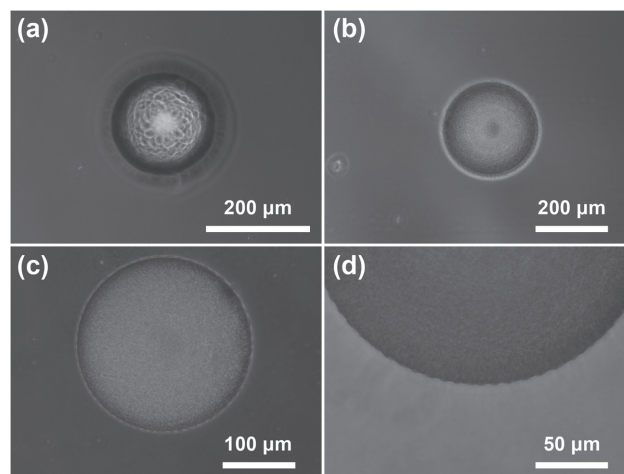


Figure 4. Optical microscope image of organic solvent droplets (PLGA:PCL-*b*-mPEG in 7:3 weight ratio dissolved in DCM) when placed in a) 1 wt% PVA aqueous solution or b,c,d) the mixture of ethanol and 1 wt% PVA aqueous solution (6:4 v/v). Ethanol was used to facilitate the formation of the stiff surface layer. The image was taken a) right after the oil droplets introduced into the aqueous phase, b) after 10 s, and c) after 30 s. d) Magnified image of (c) ($\times 2$).

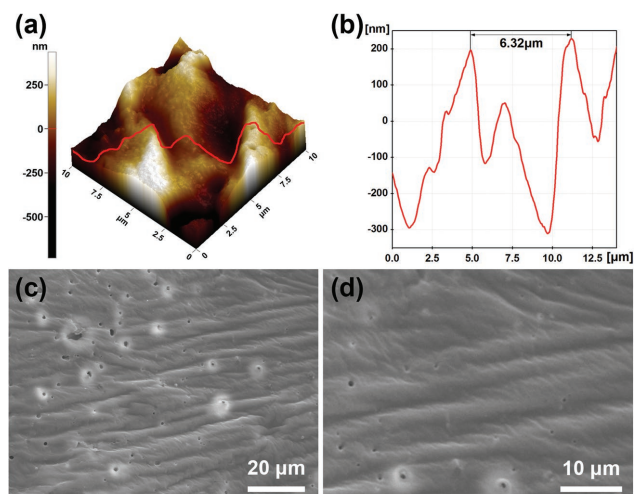


Figure 5. a) AFM image of the wrinkled surface of PLGA:PCL-*b*-mPEG film (8:2 weight ratio). b) Roughness profile of the wrinkled region. c,d) SEM images (at different magnifications) of the wrinkled surface.

release into the aqueous phase (Figure 4a), which is different from the case of PLGA alone dissolved in droplets (Figure S3, Supporting Information). This is because the different polymer chains move during the evaporation of the solvent due to the phase separation. PLGA is an amorphous biodegradable polymer while PCL is a semicrystalline biodegradable polymer, and the blends of these two polymers exhibit immiscibility.^[22] Unlike the case of wrinkle-free particles formed from PLGA alone, the wavy surface formed with the blends here is due to the combined effects of hydrophobic polymer/amphiphilic block copolymer phase separation and the trend of amphiphilic copolymer to move toward the surface of organic droplet.

Phase separation in oily droplets is kinetically governed by the evaporation of the solvent. Because the wrinkled

microparticles are prepared using only 1 wt% PVA aqueous solution as a water phase, slow evaporation at the interior of organic phase can induce complete phase separation in our microparticle fabrication method.

Furthermore, we prepared 2D film using a PLGA/PCL-*b*-mPEG blend to compare with the wrinkled particles prepared from the same blend ratio. Use of a stainless steel pan inside the Petri dish was effective for preparing well-wrinkled film that cannot be easily obtained by only using glass Petri dish (Figures S4 and S5, Supporting Information).

The phase separation creates different compositions at the surface and interior of the organic phase containing blended PLGA and PCL-*b*-mPEG. This change leads to different amounts of shrinkage and thereby forms the wrinkles. Labyrinthine phase wrinkles were also observed on the 2D films prepared with polymer blends (Figure 5).

The intervals between the wrinkles on the 2D films correspond to a wrinkle wavelength of around 6 μm. This is smaller than the value found on microparticles prepared with the same blend composition (Figure S6, Supporting Information). This may be due to the difference in the surface area of the outer layer compared with the inner soft region of the flat and curved structure.

The mechanism of wrinkle formation during the microparticle preparation by oil-in-water (O/W) solvent evaporation is proposed in Figure 6. After the organic droplets are placed in the aqueous phase, the solvent in the droplets evaporates with time from the interfacial region to generate a stiff surface layer. At the same time, the amphiphilic copolymer in the inner region migrates toward the surface. This is evidenced by interfacial tension lowering effect^[25] with the introduction of amphiphilic block copolymer which was shown in Figure 3. Thus, some of amphiphilic copolymer participates in forming a stiff layer at the interface and the remaining is located in the droplets beneath the stiff layer. As the solvent continues to evaporate and leaves the organic droplet, the radius of the droplet

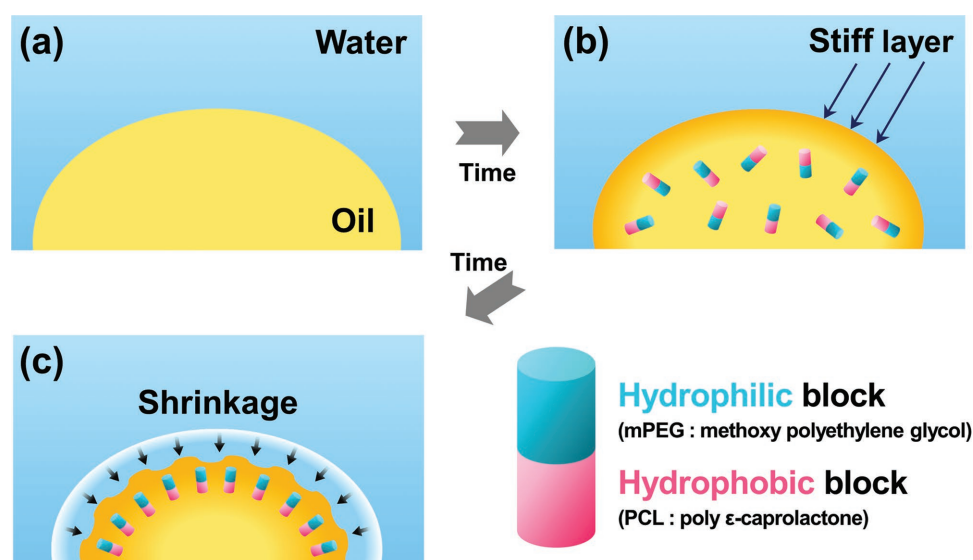


Figure 6. Schematic of labyrinthine wrinkle formation on the surface of organic droplet that contains PLGA:PCL-*b*-mPEG blend where the amount of amphiphilic block copolymer exceeds 20 wt%.

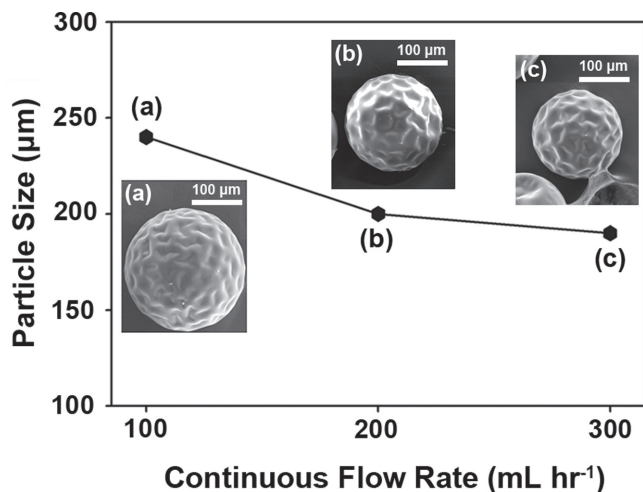


Figure 7. Effect of continuous flow rate ($\text{mL}\cdot\text{h}^{-1}$) on the size of the wrinkled microparticle. Blend ratio of PLGA/PCL-*b*-mPEG is 8:2. Discontinuous flow rate is fixed to $0.1 \text{ mL}\cdot\text{h}^{-1}$.

is reduced, which generates a compressive force in the bilayer (stiff layer on soft substrate), and the resulting buckling of the thin surface layer causes the wrinkling.

Recently, hemispherical^[13] and spherical balls^[12] made of deformable silicone-based elastomer, with radius $R = 20.0 \text{ mm}$ and various skin layer thicknesses of (h), were designed by other research groups to investigate the surface pattern formation. These spheres were hollow inside, and a pneumatic device was applied to control the interior cavity pressure (p_i). When the stress in the skin layer (adjusted by the pressure difference $\Delta p = p_a - p_i$, with p_a being the atmospheric pressure) reaches a critical value, which is sensitive to the shell thickness and mechanical properties of the sphere, the sphere bifurcates into a periodically dimple structure in order to release circumferential compression in the shell. As the shrinkage further increases, a second bifurcation (wrinkle-to-fold) takes place, breaking the dimples into fold-like structures.^[11]

In our system, the stress due to the droplet size reduction through the evaporation of the DCM solvent corresponds to Δp in the pneumatically driven elastomer system. The diameters of the initial organic droplet and final microparticle differ by almost $100 \mu\text{m}$ (Figure S7, Supporting Information). Thus, the appearance of the labyrinthine phase on the surface of microparticles shown in Figure 1 indicates a high stress is applied on the stiff layer during solidification of the droplet.

Aside from the stress, the R/h ratio (R being the radius of the particle) also affects the surface wrinkle pattern, which changes from the dimpled to labyrinthine with increasing R/h value.^[12] The critical R/h value has been reported to be 100 .^[19]

In our case, the microparticle size could be controlled with the aqueous continuous flow rate with in the tube-type fluidic device.^[23] This is also applicable to the wrinkled microparticles based on the blend of hydrophobic and amphiphilic block copolymer (Figure 7). Specifically, at higher continuous flow rates, smaller organic droplets are released from the needle, resulting in smaller wrinkled particles (lower R). Assuming that the value of h remains the same,^[28] the R/h value is lower in smaller organic droplets. Thus, the surface wrinkles changed

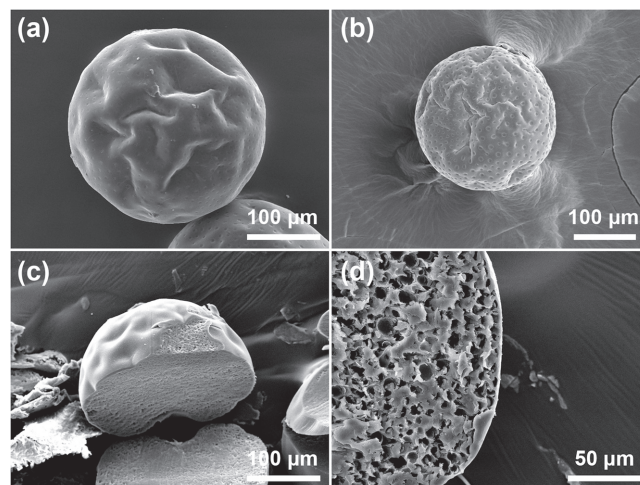


Figure 8. Dual-wrinkled microparticles a) and b) PLGA/PCL-*b*-mPEG copolymer (8:2 based on wt%). Cross-sectional SEM image of c) wrinkled (labyrinthine phase) and d) dual-wrinkled microparticles.

from the labyrinthine pattern to bistable phase, which is intermediate of labyrinthine and hexagonal phases. Similar effects of R on the pattern selection were also reported in previous works (Ag core/ SiO_2 shell system with $R = 3.0$ and $7.0 \mu\text{m}$).^[5]

Although further increase of the continuous flow rate to achieve hexagonal wrinkle phase was limited due to the difficulty in preparing uniformly sized particles at current stage. It is noteworthy that the pattern change observed here with changing R can be compared with the recently reported elastomer sphere system controlled by the pneumatic device.

Previously, we had succeeded in the fabrication of golf-ball-patterned microparticles, which is hexagonal phase on the surface using various homopolymers.^[23] By combining the methods of using inert organic PCMs for preparing dimple structure and using PLGA/PCL-*b*-mPEG copolymer blend, we successfully prepared dual-wrinkled microparticles that simultaneously possess both labyrinthine and hexagonal phases for the first time (Figure 8a,b). Here, a dual-wrinkled pattern is clearly different from the bistable phase (intermediate coexistence phase) that covers the surface by either dimples or labyrinthine patterns. It is anticipated that prepared microparticles can be applied to various fields including biomedical application owing to the use of biocompatible moieties. The dual-wrinkled patterns permit multiscaled interfacial roughness.

Because of the use of biocompatible moieties, such microparticles can be used in various biomedical applications. To investigate the general applicability of this approach, we also fabricated dual-wrinkled microparticles using other biocompatible polymer blends of a homopolymer and an amphiphilic block copolymer. Successful results are obtained for two different blends: PLGA/PDLA-*b*-mPEG and PLGA/PCL-*b*-PCL (Figures S8–S10, Supporting Information), as shown in Figure 9. PLGA and PDLA are amorphous polymers, whereas PCL is a semicrystalline polymer. More corrugated surfaces were observed for the blend containing PCL moieties, because the semicrystalline polymer displayed larger volume change than the amorphous phase during solidification. It is also possible that a thicker stiff layer was formed for PLGA blended with

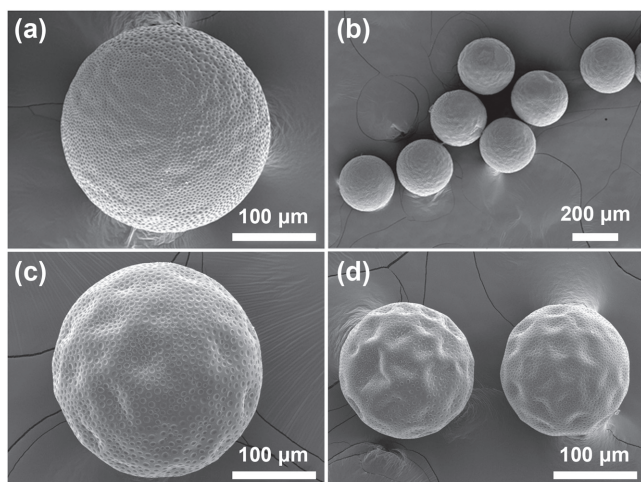


Figure 9. SEM images of the dual-wrinkled microparticles from a, b) PLGA/PDLA-*b*-mPEG blend and c, d) PLGA/PCL-*b*-PEG-*b*-PCL blend. Blend ratio of PLGA: amphiphilic copolymer was 8:2 based on weight.

PCL-*b*-mPEG or PCL-*b*-PEG-*b*-PCL compared to PDLA-*b*-mPEG because the amplitude of the wrinkle depends on the thickness of stiff layer *h* as well as on the applied strain.^[29]

4. Conclusion

Inspired by different wrinkle patterns on the surface of natural particles, especially biological ones, we have created microparticles with dual-wrinkled surface, utilizing the surface instability mechanism both from the hydrophobic polymer/amphiphilic block copolymer blend and by incorporation of organic PCMs. Our new approach realized both labyrinthine and hexagonal phases on the same surface of microparticles for the first time.

It is also noteworthy that the polymer materials in the microparticles are biocompatible and biodegradable, and the synthesized microparticles have uniform sizes. Hence, these particles can have potential biomedical uses that could not be easily obtained from conventional wrinkled microparticles from elastomeric or crosslinked polymers.

Furthermore, this approach based on hydrophobic polymer/amphiphilic block copolymer blends could be extended to other blend systems for a wider range of applications.

Supporting Information

Supporting Information is available from the Wiley Online Library or from the author.

Acknowledgements

J.I. and D.Y. contributed equally to this work. This work was supported by the research fund of Hanyang University (HY-2015-2121).

Conflict of Interest

The authors declare no conflict of interest.

Keywords

amphiphilic block copolymer, microfluidics, microparticles, surface instability, wrinkling

Received: March 22, 2017

Revised: May 16, 2017

Published online: July 19, 2017

- [1] S. Mitragotri, J. Lahann, *Nat. Mater.* **2009**, *8*, 15.
- [2] B. Li, Y.-P. Cao, X.-Q. Feng, H. Gao, *Soft Matter* **2012**, *8*, 5728.
- [3] J. C. Brasen, L. F. Olsen, M. B. Hallett, *Cell Calcium* **2010**, *47*, 339.
- [4] M. A. García, B. Galati, A. Anton, *Bot. J. Linn. Soc.* **2002**, *139*, 383.
- [5] G. Cao, X. Chen, C. Li, A. Ji, Z. Cao, *Phys. Rev. Lett.* **2008**, *100*, 036102.
- [6] N. Bowden, S. Brittain, A. G. Evans, J. W. Hutchinson, G. M. Whitesides, *Nature* **1998**, *393*, 146.
- [7] E. P. Chan, A. J. Crosby, *Adv. Mater.* **2006**, *18*, 3238.
- [8] H. J. Bae, S. Bae, C. Park, S. Han, J. Kim, L. N. Kim, K. Kim, S. H. Song, W. Park, S. Kwon, *Adv. Mater.* **2015**, *27*, 2083.
- [9] D. Terwagne, M. Brojan, P. M. Reis, *Adv. Mater.* **2014**, *26*, 6608.
- [10] H.-K. Chan, *Expert Opin. Drug Delivery* **2008**, *5*, 909.
- [11] B. Li, F. Jia, Y.-P. Cao, X.-Q. Feng, H. Gao, *Phys. Rev. Lett.* **2011**, *106*, 234301.
- [12] N. Stoop, R. Lagrange, D. Terwagne, P. M. Reis, J. Dunkel, *Nat. Mater.* **2015**, *14*, 337.
- [13] M. Brojan, D. Terwagne, R. Lagrange, P. M. Reis, *Proc. Natl. Acad. Sci. USA* **2015**, *112*, 14.
- [14] V.-T. Tran, J.-P. Benoît, M.-C. Venier-Julienne, *Int. J. Pharmacol.* **2011**, *407*, 1.
- [15] J. Rodríguez-Hernández, *Prog. Polym. Sci.* **2015**, *42*, 1.
- [16] J. Yin, X. Han, Y. Cao, C. Lu, *Sci. Rep.* **2014**, *4*, 5710.
- [17] H.-G. Park, H.-C. Jeong, Y. H. Jung, D.-S. Seo, *Sci. Rep.* **2015**, *5*, 12356.
- [18] A. C. Trindade, J. P. Canejo, P. Patrício, P. Brogueira, P. I. Teixeira, M. H. Godinho, *J. Mater. Chem.* **2012**, *22*, 22044.
- [19] A. Trindade, J. P. Canejo, L. Pinto, P. Patrício, P. Brogueira, P. I. C. Teixeira, M. Godinho, *Macromolecules* **2011**, *44*, 2220.
- [20] T. Nisisako, T. Torii, *Adv. Mater.* **2007**, *19*, 1489.
- [21] D. Dendukuri, D. C. Pregibon, J. Collins, T. A. Hatton, P. S. Doyle, *Nat. Mater.* **2006**, *5*, 365.
- [22] S. W. Kim, K.-H. Hwangbo, J. H. Lee, K. Y. Cho, *RSC Adv.* **2014**, *4*, 46536.
- [23] K.-H. Hwangbo, M. R. Kim, C.-S. Lee, K. Y. Cho, *Soft Matter* **2011**, *7*, 10874.
- [24] G. Gompper, M. Schick, *Phys. Rev. Lett.* **1990**, *65*, 1116.
- [25] J. Zhu, R. C. Hayward, *J. Am. Chem. Soc.* **2008**, *130*, 7496.
- [26] S. Liu, R. Deng, W. Li, J. Zhu, *Adv. Funct. Mater.* **2012**, *22*, 1692.
- [27] Z. Huang, W. Hong, Z. Suo, *J. Mech. Phys. Solids* **2005**, *53*, 2101.
- [28] H. Katou, A. J. Wandrey, B. Gander, *Int. J. Pharmacol.* **2008**, *364*, 45.
- [29] S. Yang, K. Khare, P. C. Lin, *Adv. Funct. Mater.* **2010**, *20*, 2550.